1 December 1996

OPTICS COMMUNICATIONS

ELSEVIER

Optics Communications 132 (1996) 343–352

Full length article

Wigner distribution function for paraxial polychromatic optics

Kurt Bernardo Wolf [1]

Centro Internacional de Ciencias AC, Apartado Postal 48-3, 62251 Cuernavaca, Morelos, Mexico

Received 21 February 1996; accepted 4 June 1996

Abstract

Polychromatic paraxial wavefields and their color images on a screen are provided here with a Wigner distribution function of position, momentum and wavelength. The definition is based on the Heisenberg–Weyl group. In the monochromatic limit we return to the common Wigner function and phase-space formalism. We examine one- and two-Gaussian polychromatic wavefields.

1. Introduction

The Wigner distribution function and phase-space formalism was developed by L. Szilard and E.P. Wigner [1]. It has been applied extensively in quantum mechanics [2,3], quantum optics [4] and signal analysis [5]. In the latter, when used for paraxial images, light must be assumed monochromatic for the current formalism to apply. Our objective here is to include the wavelength among the classical variables of a generalized Wigner function which we propose based on harmonic analysis on the full Heisenberg–Weyl group.

In quantum mechanics, the fundamental constant which provides the scale between the canonically conjugate coordinates of position and momentum in the Planck constant h; in optics, it is the wavelength λ. The former is evidently fixed, but the latter is not. For two wavefunctions f and g, we recall the definition of their *Wigner distribution function* (of classical 'c-number' coordinates of position and momentum) given by

$$F_{f,g}^{W,\hbar}(q,p)=\frac{1}{2\pi\hbar}\int_{\mathscr{R}}\mathrm{d}x\,f\left(q-\tfrac{1}{2}x\right)^{*}\mathrm{e}^{-\mathrm{i}xp/\hbar}\times g\left(q+\tfrac{1}{2}x\right) \tag{1a}$$

$$=\frac{1}{2\pi\hbar}\int_{\mathscr{R}}\mathrm{d}y\,\tilde{f}\left(p-\tfrac{1}{2}y\right)^{*}\mathrm{e}^{+\mathrm{i}qy/\hbar}\times\tilde{g}\left(p+\tfrac{1}{2}y\right), \tag{1b}$$

where $\hbar=h/2\pi$ is the reduced Planck constant, and

$$\tilde{f}(p)=\mathscr{F}_{q\to p/\hbar}f=\frac{1}{\sqrt{2\pi\hbar}}\int_{\mathscr{R}}\mathrm{d}q\,f(q)\mathrm{e}^{-\mathrm{i}qp/\hbar} \tag{1c}$$

is the Fourier transform wavefunction of momentum. Most commonly it is used for $f=g$ as the phase-space quasiprobability distribution of the quantum system in the state f. For brevity we shall refer to this and to our ensuing generalization simply as *the* Wigner function.

[1] On sabbatical leave from Instituto de Investigaciones en Matemáticas Aplicadas y en Sistemas, Universidad Nacional Autónoma de México, Cuernavaca, Mexico.

PII S0030-4018(96)00364-1

In Section 2 we evince that paraxial polychromatic wavefields carry at least *two* signals in juxtaposition. In Section 3 we use the Heisenberg–Weyl group and operator ring [6] to define a general Wigner function; its application to such wavefields occupies Section 4. Section 5 examines the form of the Wigner function for color images on a screen and Section 6 for wavefunctions of color and momentum, where the juxtaposition problem is clarified. Section 7 analyzes the three marginal distributions (projections) which are extreme cases of the three local spectra of position, momentum (space frequency) and color. Section 8 examines the Wigner function for Gaussian-chromatic wavefields of Gaussian waist. Finally, Section 9 presents some conclusions and a wider context for application of the Wigner function in optical models.

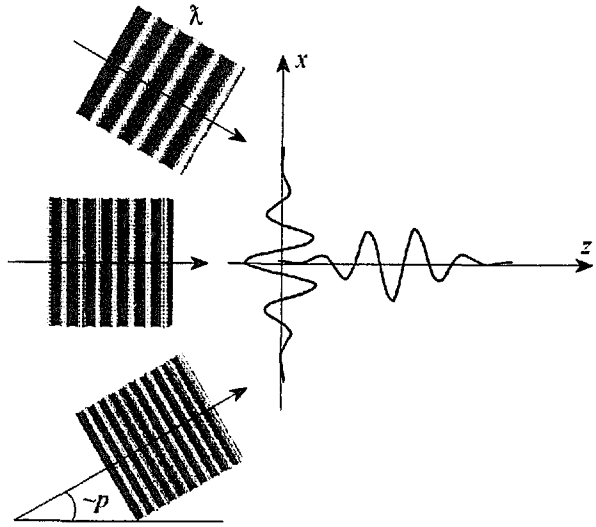

Fig. 1. A paraxial wavefield is a linear combination of plane waves in all paraxial directions p and with all (nonzero) wavelengths $\lambda = 2\pi\bar\lambda$. At least two signals are encoded: one along the optical axis z due to superposition of wavenumbers $1/\lambda$, and one on the screen x due to superposition of p/λ. The first signal juxtaposes on the second. The task is to separate them.

2. Paraxial polychromatic wavefields

We use the common optical coordinates $(x, z) \in \mathscr{R}^2$, where x is the coordinate up the screen and the optical (or 'evolution') axis z extends to the right. Paraxial plane waves of real reduced wavelength $\bar\lambda = \lambda/2\pi \neq 0$ and of momentum $p \in \mathscr{R}$ are

$$\psi^{W}_{p,\bar\lambda}(x, z) = (2\pi)^{-1} e^{i(z-xp)/\bar\lambda}. \tag{2}$$

The set of plane waves $(p, \bar\lambda)$ is Dirac-orthonormal and complete with respect to the measures $dx\,dz$ and $d(-p/\bar\lambda)\,d(1/\bar\lambda) = \bar\lambda^{-3}\ dp\ d\bar\lambda$. (Units of length are assumed for $\bar\lambda$, z and x, while p has no units.) In geometric optics, momentum p in a medium of refractive index n is related to ray inclination θ by $p = n \sin\theta$. To use the Fourier transform and canonical phase space for linear optical maps, the *paraxial model* assumes $p \in \mathscr{R}$.

A paraxial wavefield $f(x, z)$ is a generalized linear superposition of all paraxial plane waves. See Fig. 1. Fourier analysis shows that at least two distinct signals can be encoded in such a wavefield:

(1) $Z(z)$ on the optical axis $z \in \mathscr{R} (x = 0)$, by superposition of wavenumbers $\kappa = 1/\bar\lambda \in \mathscr{R}$ through the Fourier transform $\tilde{Z}(\kappa) = \mathscr{F}_{z \mapsto \kappa} Z$. Wavenumber κ and coordinate z are momentum and position coordinates for a phase space where the constant $\hbar$ in Eq. (1) is unity. There applies the standard Wigner function treatment of signals in the $(z, \bar\lambda^{-1})$ plane.

(2) $X(x)$ on the screen $x \in \mathscr{R}$ $(z = 0)$, by superposition of plane waves of ratio $r = p/\bar\lambda \in \mathscr{R}$ through the Fourier transform $\tilde{X}(r) = \mathscr{F}_{x \mapsto r} X$. This is the subject of paraxial imaging devices. In monochromatic wavefields, the Wigner function (1) applies and so does the associated phase-space formalism with $\hbar$ replaced by $\bar\lambda$.

The two signals, $Z(z)$ and $X(x)$, are *not* on the same footing: the first is impervious to the paraxial angular spread of the beam, while the second is conditioned by spreading of the first; i.e. the two signals are juxtaposed. Rather than solve the problem in ad hoc manner, we base our considerations on the mother symmetry of the paraxial polychromatic model of wavefields [7] to propose a proper Wigner function of position, momentum, *and* wavelength. The gained generality permits the analysis of further optical and acoustical models that will be presented elsewhere. Technically, Fourier analysis suffices to separate them and obtain results; the reader interested only in applications may skip the following text up to Eq. (19), which defines the Wigner function on a color screen, and then to Section 8, where Gaussian beams and the so-called Schrödinger cat phenomenon are examined.

3. Wigner function on the Heisenberg–Weyl group

A homogeneous and isotropic two-dimensional optical medium has manifest invariance under translations and rotations, i.e. under the group of Euclidean rigid motions [7]. Indeed, the invariance defines such a medium. The limit of small angles contracts the Euclidean group to the Heisenberg–Weyl group, which is the foundation of quantum mechanics [6].

The Heisenberg–Weyl group has three Lie generators: Q is the contracted rotation, P generates translations in the screen coordinate x, and Λ is the contracted translation along the optical axis. Independently of their realization, the commutation relations of the generators are

$$[Q, P] = \mathrm{i}\Lambda, \quad [\Lambda, Q] = 0, \quad [\Lambda, P] = 0. \tag{3}$$

The irreducible representations of the group are classified by the central generator Λ and labelled uniquely by its real eigenvalues λ.

The elements of the Heisenberg–Weyl group W are the formal exponentials

$$\begin{aligned}\omega(\xi, \eta, \zeta) &= \exp(\mathrm{i}(\xi Q + \eta P + \zeta\Lambda)) \\ &= \mathrm{e}^{\mathrm{i}\xi Q}\mathrm{e}^{\mathrm{i}\eta P}\mathrm{e}^{\mathrm{i}(\zeta + \frac{1}{2}\xi\eta)\Lambda} \\ &= \mathrm{e}^{\mathrm{i}\eta P}\mathrm{e}^{\mathrm{i}\xi Q}\mathrm{e}^{\mathrm{i}(\zeta - \frac{1}{2}\xi\eta)\Lambda}.\end{aligned} \tag{4}$$

This polar form provides coordinates $(\xi, \eta, \zeta) \in \mathscr{R}^3$ for the group elements; the group product law obtained from Eq. (3) is

$$\begin{aligned}&\omega(\xi_1, \eta_1, \zeta_1)\,\omega(\xi_2, \eta_2, \zeta_2) \\ &\quad = \omega\big(\xi_1 + \xi_2, \eta_1 + \eta_2, \\ &\qquad\qquad \zeta_1 + \zeta_2 + \tfrac{1}{2}[\eta_1\xi_2 - \xi_1\eta_2]\big).\end{aligned} \tag{5}$$

The group identity is $\omega_0 = \omega(0, 0, 0)$ and the inverse of $\omega(\xi, \eta, \zeta)$ is $\omega^{-1}(\xi, \eta, \zeta) = \omega(-\xi, -\eta, -\zeta)$. The invariant (Haar) measure on W is $\mathrm{d}\omega = \mathrm{d}\xi\,\mathrm{d}\eta\,\mathrm{d}\zeta$ and the natural Hilbert space is $\mathscr{L}_2(\mathscr{R}^3)$, with the inner product $(f, g)_W = \int_W \mathrm{d}\omega\, f(\omega)^* g(\omega)$ for functions on the group $f(\omega) = f(\xi, \eta, \zeta)$. There applies right group action ω': $f(\omega) \mapsto f(\omega\omega')$. These maps can be extended linearly to integral operators $\mathscr{A} = \int_W \mathrm{d}\omega\, A(\omega)\omega$, subject to linear combination and product, but do not necessarily have an inverse; such operators belong to a structure called the 'Heisenberg–Weyl ring' [6]. A ring element is characterized by its (generalized) function on the group, $A(\omega)$.

We now consider ring elements $\mathscr{W}(v)$ whose function on the group is

$$\begin{aligned}W(v;\omega) &= W(q, p, l; \xi, \eta, \zeta) \\ &= \exp[-\mathrm{i}(\xi q + \eta p + \zeta l)],\end{aligned} \tag{6}$$

where $v = (q, p, l) \in \mathscr{R}^3$ are three classical variables (real 'c-numbers'). (Note that ξ and ζ are implied to have units of inverse length and η has no units.) With Eq. (6) we build the formal operator

$$\begin{aligned}&\mathscr{W}(q, p, l) \\ &\quad = \int_{\mathscr{R}} \mathrm{d}\xi \int_{\mathscr{R}} \mathrm{d}\eta \int_{\mathscr{R}} \mathrm{d}\zeta \\ &\qquad \times \exp\{\mathrm{i}[\xi(Q - q) + \eta(P - p) + \zeta(\Lambda - l)]\}.\end{aligned} \tag{7}$$

(The operator is *formal* because we have not yet specified its domain of functions.) In this way we set q, p and l in correspondence with the generators Q, P and Λ of the Heisenberg–Weyl group.

There is always the natural Hilbert space $\mathscr{L}_2(\mathscr{R}^3)$ of functions on the group. On this function domain we define the Wigner function (on the group W) as the sesquilinear form of Eq. (7),

$$\begin{aligned}W^W_{f,g}(v) &= (f, \mathscr{W}(v) : g)_W \\ &= \iint_W \mathrm{d}\omega\,\mathrm{d}\omega'\, f(\omega)^* \\ &\quad \times W(v; \omega^{-1}\omega')\, g(\omega') \\ &= \iint_W \mathrm{d}\omega\,\mathrm{d}\omega'\, f(\omega'\omega^{-1/2})^* \\ &\quad \times W(v, \omega)\, g(\omega'\omega^{1/2}).\end{aligned} \tag{8}$$

The form is Hermitian because $W^W_{f,g}(v)^* = W^W_{g,f}(v)$. In the polar parametrization (4), group elements have well-defined and unique square roots $\omega(\xi, \eta, \zeta)^{1/2} = \omega(\frac{1}{2}\xi, \frac{1}{2}\eta, \frac{1}{2}\zeta)$. Specifically for the Heisenberg–Weyl case,

$$\begin{aligned}&W^W_{f,g}(q, p, l) \\ &\quad = \frac{1}{(2\pi)^3}\int_{\mathscr{R}^3} \mathrm{d}\xi\,\mathrm{d}\eta\,\mathrm{d}\zeta \int_{\mathscr{R}^3} \mathrm{d}\xi'\,\mathrm{d}\eta'\,\mathrm{d}\zeta' \\ &\qquad \times f\big(\xi - \tfrac{1}{2}\xi', \eta - \tfrac{1}{2}\eta', \\ &\qquad\qquad \zeta - \tfrac{1}{2}[\zeta' + \tfrac{1}{2}(\eta\xi' - \xi\eta')]\big)^*\end{aligned}$$

$$\times\exp[-\mathrm{i}(\xi'q+\eta'p+\zeta'l)]$$
$$\times g\big(\xi+\tfrac{1}{2}\xi',\ \eta+\tfrac{1}{2}\eta',$$
$$\zeta+\tfrac{1}{2}[\zeta'+\tfrac{1}{2}(\eta\xi'-\xi\eta')]\big). \tag{9}$$

Because of the properties of the multiple Fourier transform under linear maps of space, the vector of c-numbers $r=(q,\ p,\ \lambda\!\!\!^{-})\in\mathscr{R}^3$ and the vector of operators $(Q,\ P,\ \Lambda)$ will have the *same* transformation properties under the action of any linear transformation that preserves the commutation relations (3) (i.e. the automorphisms of its Lie algebra). They are of course invariant under W itself, but *also* under the larger group of linear (properly, symplectic) transformations [8,9]. In other words, as shown by García-Calderón and Moshinsky [10], when the fields f and g undergo the linear (integral canonical) transforms of paraxial optics, the effect on the Wigner function is a corresponding linear (classical canonical) transformation of its arguments q and p.

4. The Heisenberg–Weyl mother group of wavefields

The group W mothers a linear field model with symmetry W_s when [7]
(A) There is a standard field $f_0=f(\omega_0)$ from which all wavefields can be generated through group action, $f(\omega)=\omega$: f_0, $\omega\in W$, and (generalized) linear combination.
(B) The standard field is invariant, ω_s: $f_0=f_0$, under elements $\omega_s\in W_s\subset W$.

The standard field choosen for the paraxial wave optical model is a plane pulse along the z-axis; its symmetry are all translations *in* the x-plane of the screen, $f(\omega_0)=f(\omega_\eta)$ for $\omega_\eta=\omega(0,\ \eta,\ 0)\in W_x\subset W$. Since $f(\omega_\eta\omega)=f(\omega)$, paraxial wavefields $f(\omega)$ are constant over equivalence classes of group elements $W_x\omega$, called '(left) *cosets*'. Paraxial wavefields are thus functions on the space of left cosets $W_x\backslash W$. In the polar coordinates, Eq. (5), $\omega(\xi,\ \eta,\ \zeta)=\omega(0,\ \eta,\ 0)\omega(\xi,\ 0,\ \zeta-\frac{1}{2}\xi\eta)$, and hence [6]

$$f(\omega)=f(\xi,\eta,\zeta)=f(\xi,0,\tau)=f^{\mathrm{c}}(\xi,\tau),$$
$$\tau=\zeta-\tfrac{1}{2}\xi\eta \tag{10}$$

leads to the (transitive and effective) group action

$$\omega':f^{\mathrm{c}}(\xi,\tau)\mapsto f^{\mathrm{c}}\big(\xi+\xi',\ \tau+\zeta'-\tfrac{1}{2}\xi'\eta'-\xi\eta'\big). \tag{11}$$

(Both ξ and τ have units of inverse length. We indicate by primes those group elements whose coordinates are primed. Below we interpret the coset coordinates $(\xi,\ \tau)\in\mathscr{R}^2$.)

On the domain of (generalized) functions on the coset space $W_x\backslash W$, the Wigner function is obtained replacing Eq. (11) in the six-fold integral (9). We may extract the empty integration factor $\mathrm{Vol}\,W_x=\int_{\mathscr{R}}\mathrm{d}\eta$ and retain the five-fold integral that we call the Wigner function on the space of cosets $W_x\backslash W$. We denote it simply by $W_{f,g}(q,\ p,\ l)$, understanding that it applies to the paraxial polychromatic model of this paper. Various changes of variable such as $v=\tau-\frac{1}{8}\xi'\eta'$ allow us to collect a factor $\int_{\mathscr{R}}\mathrm{d}\eta'\ \mathrm{e}^{-\mathrm{i}(p+\xi l)\eta'}=2\pi\delta(p+\xi l)$ and eliminate another integral. The result is the Wigner function in the form

$$W_{f,g}(q,\ p,\ l)=\frac{1}{4\pi^2 l}\int_{\mathscr{R}^3}\mathrm{d}\tau\ \mathrm{d}\xi'\ \mathrm{d}\tau'$$
$$\times f^{\mathrm{c}}\big(-p/l-\tfrac{1}{2}\xi',\ \tau-\tfrac{1}{2}\tau'\big)^*$$
$$\times\exp\big[-\mathrm{i}(\xi'q+\tau'l)$$
$$\times g^{\mathrm{c}}\big(-p/l+\tfrac{1}{2}\xi',\ \tau+\tfrac{1}{2}\tau'\big)\big]. \tag{12}$$

Comparing with Eq. (1b), we identify the coset coordinate ξ with $-p/l$.

A wavefield is monochromatic (cf. Eq. (2)) when the dependence on τ is $\sim\mathrm{e}^{\mathrm{i}\tau\lambda\!\!\!^{-}_0}=\mathrm{e}^{\mathrm{i}z/\lambda\!\!\!^{-}_0}$, times an arbitrary function of ξ,

$$f^{\mathrm{c}}_{\lambda\!\!\!^{-}_0}(\xi,\tau)=\tilde{f}(-\xi)\frac{1}{\sqrt{2\pi}}\exp(\mathrm{i}\tau\lambda\!\!\!^{-}_0)$$
$$=\tilde{f}(p/\lambda\!\!\!^{-}_0)\frac{1}{\sqrt{2\pi}}\exp^{(\mathrm{i}\tau\lambda\!\!\!^{-}_0)}. \tag{13}$$

Between two monochromatic wavefields f and g, of wavelengths $\lambda\!\!\!^{-}_f$ and $\lambda\!\!\!^{-}_g$ respectively, the Wigner function (12) has two Dirac δ factors,

$$W^{\lambda\!\!\!^{-}_f,\lambda\!\!\!^{-}_g}_{f,g}(q,\ p,\ l)=\delta(l-\lambda\!\!\!^{-}_f)\delta(l-\lambda\!\!\!^{-}_g)$$
$$\times\frac{1}{2\pi l}\int_{\mathscr{R}}\mathrm{d}\xi\ \tilde{f}\big(p/l-\tfrac{1}{2}\xi\big)$$
$$\times\mathrm{e}^{\mathrm{i}q\xi}\tilde{g}\big(p/l+\tfrac{1}{2}\xi\big). \tag{14}$$

The integral is precisely the common Wigner function $F_{f,g}^{W,l}(q, p)$ in Eq. (1) (after replacement $\tilde{f}(p/l) \mapsto \sqrt{l}\tilde{f}(p)$, $\xi \mapsto y/l$, and $l \mapsto \hbar$, and understanding that the tilde means that there is a function $f(x)$ on the screen whose Fourier transform is the momentum wavefunction $\tilde{f}(p/l)$).

We have thus reduced the Wigner function on the group to the Wigner function on the coset space of the polychromatic paraxial model, and shown that in the monochromatic case it reduces to the common phase-space Wigner function.

5. Polychromatic functions on the screen

For functions on manifold $(\xi, \tau) \in \mathscr{R}^2$ of cosets we consider the natural Hilbert space $\mathscr{L}_2(\mathscr{R}^2)$ with measure $d\xi\, d\tau$ inherited from the invariant measure on the group. The group action (11) now leads to the realization of the Heisenberg–Weyl generators by (essentially self-adjoint) operators:

$$Q^c = -i\frac{\partial}{\partial \xi}, \quad P^c = i\xi\frac{\partial}{\partial \tau}, \quad \Lambda^c = -i\frac{\partial}{\partial \tau}. \qquad (15)$$

Eigenfunctions of the operators Q, P or Λ, are wavefields which can be conveniently labelled by their eigenvalues; the eigenvalues are real and provide the physical coordinates of position, momentum, or wavelength, respectively. We may choose for this purpose at most two commuting operators. Let them first be the screen coordinate q of Q and reduced wavelength $\lambda\!\!\!^{-}$ of Λ (*color*), obtained by the double Fourier transformation

$$\begin{aligned} f^s(x, \lambda\!\!\!^{-}) &= \mathscr{F}_{\xi \to x}\mathscr{F}_{\tau \to \lambda\!\!\!^{-}} f^c \\ &= \frac{1}{2\pi}\int_{\mathscr{R}^2} d\tau\, d\xi\, f^c(\xi, \tau) \\ &\quad \times \exp[-i(x\xi + \lambda\!\!\!^{-}\tau)], \end{aligned} \qquad (16)$$

and call these '(polychromatic) screen functions'. On this space $(x, \lambda\!\!\!^{-}) \in \mathscr{R}^2$, the group action on functions is

$$\begin{aligned} \omega' : f^s(x, \lambda\!\!\!^{-}) &=: f^s_{\omega'}(x, \lambda\!\!\!^{-}) \\ &= \exp\{i[x\xi' + \lambda\!\!\!^{-}(\zeta' + \tfrac{1}{2}\xi'\eta')]\} \\ &\quad \times f^s(x + \lambda\!\!\!^{-}\eta, \lambda\!\!\!^{-}). \end{aligned} \qquad (17)$$

(Mathematically this is known as a ray representation of the Heisenberg–Weyl group, and called the Schrödinger irreducible representation for $\lambda\!\!\!^{-} = \hbar$.) Here, the generators of W are the operators

$$Q^s = x\cdot, \quad P^s = -i\lambda\!\!\!^{-}\frac{\partial}{\partial x}, \quad \Lambda^s = \lambda\!\!\!^{-}\cdot. \qquad (18)$$

On the space of color screen functions $f^s(x, \lambda\!\!\!^{-})$, the common Schrödinger formalism is thus valid for variable wavelength. Note that translations in x are generated by P, but $\lambda\!\!\!^{-}$ cannot be translated within W. The three coordinates (q, p, l) in the Wigner function are by no means those of an ordinary Euclidean vector space; the first two are of phase space and the third is their fundamental scale 'constant'. (Group theoretically, q and p are row labels and l labels the irreducible representation; the set is complete.)

The paraxial polychromatic Wigner function (12) can be written with screen functions, (16), as

$$\begin{aligned} W_{f,g}(q, p, l) &= \frac{1}{2\pi l}\int_{\mathscr{R}} dx\, f^s(q - \tfrac{1}{2}x, l)^* \\ &\quad \times e^{-ixp/l} g^s(q + \tfrac{1}{2}x, l), \end{aligned} \qquad (19)$$

cf. Eq. (1a). The wavelength of f^s and g^s is *not* convolved, as are q and p. Again, monochromaticity leads to two δ, times the Wigner function (1). We believe that Eq. (19) is the form best suited for its application, because usually the spectral distribution of the light source is known independently, and/or the color of the image can be sensed spectrographically.

6. Polychromatic momentum functions

Paraxial plane waves, Eq. (2), were labelled by momentum and wavelength, $(p, \lambda\!\!\!^{-}) \in \mathscr{R}^2$, $\lambda\!\!\!^{-} \neq 0$. The Fourier transform of the coset functions, or inverse Fourier transform of the color screen functions yields

$$\begin{aligned} f^m(\xi, \lambda\!\!\!^{-}) &= \mathscr{F}_{\tau \to \lambda\!\!\!^{-}} f^c(\xi) \\ &= \frac{1}{\sqrt{2\pi}}\int_{\mathscr{R}} d\tau\, f^c(\xi, \tau) e^{-i\lambda\!\!\!^{-}\tau} \\ &= \mathscr{F}^{-1}_{\xi \to x} f^s(\lambda\!\!\!^{-}) \\ &= \frac{1}{\sqrt{2\pi}}\int_{\mathscr{R}} dx\, f^s(x, \lambda\!\!\!^{-}) e^{ix\xi}, \end{aligned} \qquad (20)$$

that we call '(polychromatic) momentum functions' on $(\xi, \lambda) \in \mathscr{R}^2$, $\lambda \neq 0$. Recall from Eq. (12) that we identify $p = -\xi\lambda$.

In the momentum realization, the group action (11)–(17) on functions is

$$\omega' : f^{\mathrm{m}}(\xi, \lambda) \mapsto f^{\mathrm{m}}_{\omega'}(\xi, \lambda) = \exp\big(\mathrm{i}\lambda(\zeta' - \tfrac{1}{2}\xi'\eta')\big) f^{\mathrm{m}}(\xi + \xi', \lambda), \tag{21}$$

and its generators are

$$Q^{\mathrm{m}} = -\mathrm{i}\frac{\partial}{\partial \xi}, \quad P^{\mathrm{m}} = -\lambda\xi\cdot, \quad \Lambda^{\mathrm{m}} = \lambda\cdot. \tag{22}$$

The Wigner function in momentum form is obtained from Eqs. (12), (19) and (20),

$$W_{f,g}(q, p, l) = \frac{1}{2\pi l}\int_{\mathscr{R}} \mathrm{d}\xi'\, f^{\mathrm{m}}\big(-p/l - \tfrac{1}{2}\xi', l\big)^* \times \mathrm{e}^{-\mathrm{i}q\xi'} g^{\mathrm{m}}\big(-p/l + \tfrac{1}{2}\xi', l\big). \tag{23}$$

(The minus sign of $p = -\xi\lambda$ is ugly, but a consequence of using consistently the definition in Eq. (1c) of momentum function; in the literature, the opposite sign is sometimes used.)

It is important to note that in the coset coordinates (ξ, λ) the invariant measure is Cartesian: $\mathrm{d}\xi\, \mathrm{d}\lambda$, whereas in the color-momentum coordinates (p, λ) it is *skew*: $\mathrm{d}\xi\, \mathrm{d}\lambda = \lambda^{-1}\mathrm{d}\lambda\, \mathrm{d}p = \mathrm{d}\ln\lambda\, \mathrm{d}p$. This is shown in Fig. 2. If by external means we can change the wavelength, as by Doppler blue or red shift [9], the momentum coordinate p and the phase space measure $\mathrm{d}q\, \mathrm{d}p$ will shrink or expand.

A wavefield F on the (x, z) optical plane is built of paraxial plane waves, Eq. (2), as

$$F(x, z) = \int_{\mathscr{R}} \mathrm{d}\xi\, \mathrm{d}\lambda\, f^{\mathrm{m}}(\xi, \lambda)\psi^{W}_{-\xi\lambda,\lambda}(x, z), \tag{24a}$$

$$f^{\mathrm{m}}(\xi, \lambda) = \frac{1}{\lambda^2}\int_{\mathscr{R}} \mathrm{d}x\, \mathrm{d}z\, F(x, z)\psi^{W}_{-\xi\lambda,\lambda}(x, z)^*. \tag{24b}$$

The problem of separation of the two juxtaposed signals in the (x, z) optical plane, addressed in Section 2, is thus solved by any function $f^{\mathrm{m}}(\xi, \lambda)$ such that $F_\Lambda(\kappa) = (2\pi)^{-1/2}\int_{\mathscr{R}} \mathrm{d}\xi\, f^{\mathrm{m}}(\xi, \kappa^{-1})$ be the Fourier transform of the signal along the optical axis $Z(z)$, and $F_\Xi(\xi) = (2\pi)^{-1/2} \times \int_{\mathscr{R}} \mathrm{d}\lambda\, f^{\mathrm{m}}(\xi, \lambda)$ be the Fourier transform of the field at the screen $X(x)$. In particular, it is solved by their product $f^{\mathrm{m}}(\xi, \lambda) = F_\Xi(\xi)F_\Lambda(\lambda^{-1})$.

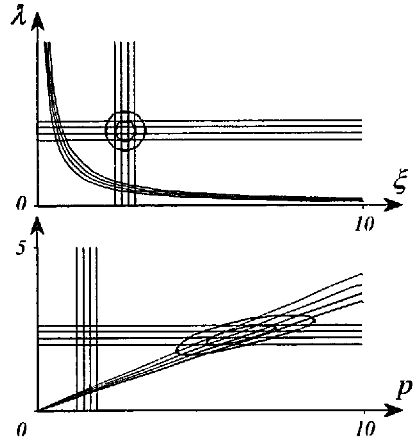

Fig. 2. Area elements and contour plots of a beam in the $\xi-\lambda$ plane (above) and its corresponding image in the $p-\lambda$ plane (below). The area element is $\mathrm{d}\xi\, \mathrm{d}\lambda$; reducing the wavelength λ will shrink momentum accordingly.

7. Marginal distributions

The Wigner function (Eq. (1) for $f = g$) gives an attractive interpretation of quantum mechanics through its marginal distributions [2,3], or projections

$$\int_{\mathscr{R}} \mathrm{d}p\, F^{W,\hbar}_{f,g}(q, p) = f(q)^*\, g(q), \tag{25a}$$

$$\int_{\mathscr{R}} \mathrm{d}q\, F^{W,\hbar}_{f,g}(q, p) = \hbar^{-1}\tilde{f}(p/\hbar)^*\, \tilde{g}(p/\hbar). \tag{25b}$$

The polychromatic Wigner function has the following marginal distributions for functions on the screen, Eq. (19), on momentum, Eq. (23), and on phase space, Eq. (12):

$$M^{\mathrm{s}}_{f,g}(q, l) = \int_{\mathscr{R}} \mathrm{d}p\, W_{f,g}(q, p, l) = f^{\mathrm{s}}(q, l)^*\, g^{\mathrm{s}}(q, l), \tag{26a}$$

$$M^{\mathrm{m}}_{f,g}(p,l)=\int_{\mathscr{R}}\mathrm{d}q\,W_{f,g}(q,p,l)$$
$$=l^{-1}f^{\mathrm{m}}(-p/l,l)^{*}\,g^{\mathrm{m}}(-p/l,l),\tag{26b}$$

$$M^{\mathrm{c}}_{f,g}(q,p)$$
$$=\int_{\mathscr{R}}\mathrm{d}l\,W_{f,g}(q,p,l)=\int_{\mathscr{R}}\mathrm{d}l\,F^{W,l}_{f,g}(q,p)$$
$$=\frac{1}{2\pi}\int_{\mathscr{R}}\frac{\mathrm{d}l}{l}\int_{\mathscr{R}}\mathrm{d}x\,f^{\mathrm{s}}(q-\tfrac{1}{2}x,l)^{*}$$
$$\times\mathrm{e}^{-\mathrm{i}xp/l}g^{\mathrm{s}}(q+\tfrac{1}{2}x,l)$$
$$=\frac{1}{2\pi}\int_{\mathscr{R}}\frac{\mathrm{d}l}{l}\int_{\mathscr{R}}\mathrm{d}\xi\,f^{\mathrm{m}}(-p/l-\tfrac{1}{2}\xi,l)^{*}$$
$$\times\mathrm{e}^{-\mathrm{i}q\xi}g^{\mathrm{m}}(-p/l+\tfrac{1}{2}\xi,l).\tag{26c}$$

For $f=g$, Eq. (26a) represents the intensity at each screen point and color, and Eq. (26b) its momentum and color content; as before, wavelength is unconvolved. Eq. (26c) is the simple color integral of the common monochromatic Wigner function $F^{W,\lambda}_{f,g}(q,p)$ on phase space. The total intensity of the field f on the screen, as seen by a color-blind observer, is $I^{\mathrm{s}}_f(q)=\int_{\mathscr{R}}\mathrm{d}p\,M^{\mathrm{c}}_{f,f}(q,p)=\int_{\mathscr{R}}\mathrm{d}l\,M^{\mathrm{s}}_{f,f}(q,l)$. The energy density in wavelength is $I^{\mathrm{c}}_f(l)=\int_{\mathscr{R}^2}\mathrm{d}q\,\mathrm{d}p\,W_{f,f}(q,p,l)$. Finally, the integral over all arguments ('volume' of the Wigner function) is

$$\int_{\mathscr{R}}\mathrm{d}q\int_{\mathscr{R}}\mathrm{d}p\int_{\mathscr{R}}\mathrm{d}l\,W_{f,g}(q,p,l)$$
$$=\int_{\mathscr{R}}\mathrm{d}x\int_{\mathscr{R}}\mathrm{d}\lambda\,f^{\mathrm{s}}(x,\lambda)^{*}\,g^{\mathrm{s}}(x,\lambda)$$
$$=(f,g)W_{\mathrm{s}}\backslash W.\tag{27}$$

For $f=g$ it is interpreted as the total energy in the field.

8. Gaussian polychromatic beams and cat states

It is well known that between monochromatic Gaussian beams, the Wigner function is a product of Gaussians on the phase-space plane. Now we propose beams also Gaussian in color. We consider Gaussian functions of u, with (complex) width $w=w_1+\mathrm{i}w_2$ and center $c=c_1+\mathrm{i}c_2$, defined by

$$\Gamma_{w,c}(u)=\left(\frac{1}{\pi}\mathrm{Re}\frac{1}{w}\right)^{1/4}$$
$$\times\exp\left(-\frac{(u-c_1)^2}{2w}+\mathrm{i}c_2(u-\tfrac{1}{2}c_1)\right).\tag{28}$$

The waist is $w_1>0$ and w_2 is the chirp (in units of u^2); c_1 is the center of the signal peak (of units u) and c_2 the center of the frequency peak (of units u^{-1}); the standard deviation is $\sqrt{2w}$. Normalization has been chosen such that $\int_{\mathscr{R}}\mathrm{d}u\,|\Gamma_{w,c}(u)|^2=1$ and so $\lim_{w\to0+}|\Gamma_{w,c}(u)|^2=\delta(u-c)$. The properties of a Gaussian function (28) include: the Fourier transform of a Gaussian of width w is a Gaussian of width w^{-1}; the product of two Gaussians is a Gaussian whose width is the harmonic sum of the widths; the Wigner function of a Gaussian of width w is a product of two Gaussians of widths $\frac{1}{2}w$ and $2\hbar^2/w$ in the two conjugate coordinates.

We call a beam 'Gauss-chromatic' when its screen function has the simple factored form $\sim f(x)\Gamma_{\alpha,\mu}(\lambda)$, with color (reduced wavelength) μ and width α; both can be complex. When the image $f(x)$ on the screen is *also* a Gaussian (of center c and width w), we call it a 'polychromatic Gaussian beam',

$$\Gamma^{\mathrm{s}}_{w,c;\alpha,\mu}(x,\lambda)=\Gamma_{w,c}(x)\Gamma_{\alpha,\mu}(\lambda).\tag{29a}$$

(Alternatively, this function may serve to model color Gaussian filters, used as by Lohmann in Ref. [5] to smooth out by convolution the measurements of the Wigner function by an extended sensor.) The coset and momentum forms of these beams are (from Eqs. (16) and (20)),

$$\Gamma^{\mathrm{c}}_{w,c;\alpha,\mu}(\xi,\tau)=\Gamma_{1/w,\mathrm{i}c}(\xi)\Gamma_{1/\alpha,\mathrm{i}\mu}(\tau),\tag{29b}$$

$$\Gamma^{\mathrm{m}}_{w,c;\alpha,\mu}(-p/\lambda,\lambda)$$
$$=\lambda^{1/2}\Gamma_{\lambda^2/w,\lambda c_2-\mathrm{i}c_1/\lambda}(p)\Gamma_{\alpha,\mu}(\lambda).\tag{29c}$$

The Wigner function for two different polychromatic Gaussians is found from Eqs. (12)–(29c), (19)–(29a), or (23)–(29b). It is

$$\begin{aligned} W_{\Gamma_{w,c;\alpha,\mu},\Gamma_{w',c';\alpha',\mu'}}(q,p,l) &= \frac{1}{2\pi l}\Gamma_{\alpha,\mu}(l)^{*}\,\Gamma_{\alpha',\mu'}(l) \\ &\quad\times\int_{\mathscr{R}} \mathrm{d}x\;\Gamma_{w,c}(q-\tfrac{1}{2}x)^{*}\,\mathrm{e}^{-\mathrm{i}xp/l}\,\Gamma_{w',c'}(q+\tfrac{1}{2}x) \\ &= Bl^{-1}\Gamma_{W,C}(q)\,\Gamma_{\tilde{W},\tilde{C}(q)}(p)\,\Gamma_{A,M}(l), \end{aligned} \tag{30}$$

where B is independent of (q, p, l), and the widths and complex centers, obtained as coefficients of the quadratic and linear terms of the three variables, are

$$\begin{aligned} W &= \frac{1}{4}(w^{*}+w'), \\ \frac{C_1}{W}+\mathrm{i}C_2 &= \frac{2}{w^{*}+w'}\big((c_1+c_1') \\ &\qquad +\mathrm{i}(c_2'w'-c_2w^{*})\big), \\ \tilde{W} &= \frac{l^2}{4}\left(\frac{1}{w^{*}}+\frac{1}{w'}\right), \\ \frac{\tilde{C}_1}{\tilde{W}}+\mathrm{i}\tilde{C}_2 &= \frac{2}{l}\frac{w^{*}w'}{w^{*}+w'}\left((c_2+c_2') \right.\\ &\qquad \left. +\mathrm{i}\left(\frac{q-c_1'}{w'}-\frac{q-c_1}{w^{*}}\right)\right), \\ \frac{1}{A} &= \frac{1}{\alpha^{*}}+\frac{1}{\alpha'}, \\ \frac{M_1}{A}+\mathrm{i}M_2 &= \frac{\mu_1}{\alpha^{*}}+\frac{\mu_1'}{\alpha'}+\mathrm{i}(\mu_2'-\mu_2). \end{aligned} \tag{31}$$

The linear dependence of $\tilde{C}(q)$ vanishes when $w' = w^{*}$. When $w' = w$ is real, Eqs. (31) yield the simple results

$$\begin{aligned} &W=\tfrac{1}{2}w, \quad C_1=\tfrac{1}{2}(c_1+c_1'), \quad C_2=-c_2+c_2', \\ &\tilde{W}=l^2/2w, \quad \tilde{C}_1=\tfrac{1}{2}l(c_2+c_2'), \quad \tilde{C}_2=-c_1+c_1', \\ &A=\tfrac{1}{2}\alpha, \quad M_1=\tfrac{1}{2}(\mu_1+\mu_1'), \quad M_2=-\mu_2+\mu_2'. \end{aligned} \tag{32}$$

In Fig. 3 we show the Wigner function $W_{\Gamma,\Gamma}(q, p, l)$ of a polychromatic Gaussian beam of real width as a stack of level plots. Each l = (constant slice) is a Gaussian, familiar from the common

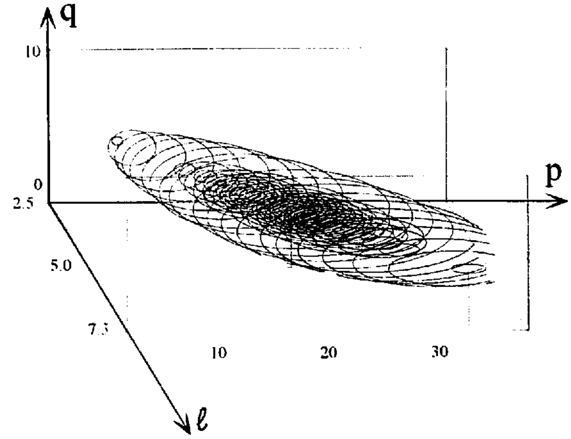

Fig. 3. Wigner function of position, momentum, and wavelength (p, q, l) for a polychromatic Gaussian beam $\Gamma^{s}_{w,c;\alpha,\mu}(x, \lambda)$ on the screen. The beam has waist $w = 2$ and (complex) center at $c = 5 + 5\mathrm{i} = q + \mathrm{i}p$; its color content is a real Gaussian centered at wavelength $\mu = 5 = l$ and width (line spread) $\alpha = 1$. The contours follow the function values 0.1, 0.2, ...

Wigner function of monochromatic optics [11], whose center is at (c_1, c_2, μ_1) as expected, and real because the frequencies C_2, $\tilde{C}_2$ and M_2 vanish. The stack tilts in the p–l plane. (In the coordinates $(q, p/l, l)$ however, the level surfaces are ellipsoids.)

In quantum optics there has been recent interest on the Wigner function for fields made up of two or more coherent Gaussian states [11]. Schrödinger's famous paradox on the quantum superposition of living and dead states of a cat has prompted these to be called 'cat states'. In the polychromatic paraxial model, cat states of the form $G(q, l) = a\Gamma(q, l) + d\Gamma'(q, l)$ have a Wigner function of the structure

$$W_{G,G} = |a|^2 W_{\Gamma,\Gamma} + |d|^2 W_{\Gamma',\Gamma'} + 2\,\mathrm{Re}\, a^{*}d\,W_{\Gamma,\Gamma'}. \tag{33}$$

As in the monochromatic case, there are two 'classical' Gaussian peaks at the centers of phase space and color of the two constituent beams. There is also a peculiar cross term whose general form is also Gaussian, and appears as a region of superoscillation between the classical peaks. The superoscillation region has acquired the name of 'smile' of the cat state; its exact nature as a quantum state of light, detectability and possible applications are still under debate [11], because the smile region smoothens when other distribution functions are used, such as the Q- or Husimi function [3] (see below); but it does not, apparently, disappear. The evolution of Gaussian coherent states in the nonlinear Kerr medium also produces resonant cat-like states at fractions and multiples of the system's cycle. The smile phenomenon is present also in the polychromatic optical model.

In Fig. 4 we show the Wigner function for color cat states with $w' = w$ real. There is a more complex three-dimensional smile region in these figures, whose oscillation frequency is contained in Eqs. (32), i.e., C_2 in q, $\tilde{C}_2$ in p, and M_2 in l. In this model it appears that the smile of cat states in (q, p, l) is related to the symmetry in the interference pattern in the (x, z) optical space, whose intensity fades out quickly as a Gaussian function of the separation between the classical states. Another implication is that if the source or sensor is not strictly monochromatic (i.e. a Lohmann Gaussian color filter), the superoscillations of the cat's smile will convolute and quickly die out.

If a Gaussian color beam is sent through a 'harmonic oscillator' optical fiber, the stack of Fig. 3 will rotate in the (q, p) plane as usual; if the refractive index of the fiber depends on wavelength however, each plane will rotate at its own frequency and the stack will shear. As the shear becomes large and parts of the beam differ by near-2π rotation, Fig. 4 indicates that there will form cat-like smile regions between them where resonances can be expected [12].

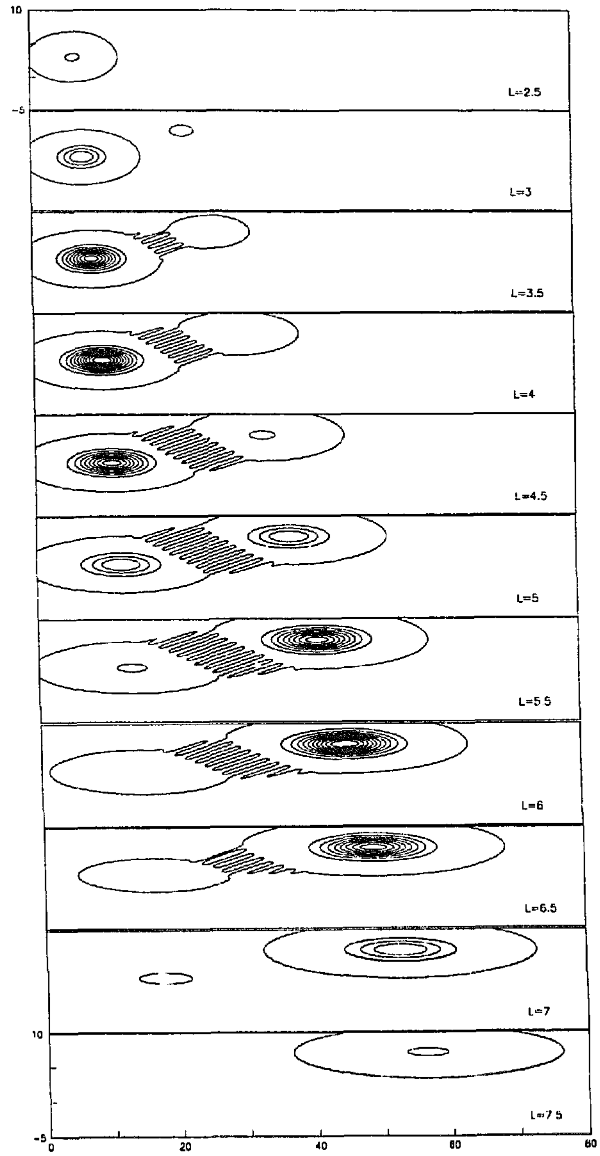

Fig. 4. Level plots of the Wigner function of a polychromatic two-Gaussian cat state for several values of the reduced wavelength $\bar{\lambda} = \lambda/2\pi$ (marked L at right) 2.5, 3.0, ..., 7.5. The two beams are polychromatic Gaussians of color (wavelength) centers $\mu = 4$ and $\mu' = 6$, and real widths (line spread) $\alpha = \alpha' = 1$. On (q, p) phase space, the Gaussian centers are at $c = 3 + 2.5i$ and $c' = 7 + 7.5i$ and have equal waist $w = w' = 2$. The region of rapid oscillation in their middle is the cat smile. The lowest contour follows the value 10^{-4} of the function; the next ones indicate values 0.1, 0.2, ...

9. Conclusions

We have proposed a correspondence, through the Wigner function, between classical observables and operators of position, momentum and wavelength, for the wavefields of paraxial polychromatic optics. Another model of interest where our methods and results apply is that of paraxial acoustics. The correspondence generalizes the phase space picture provided by the (monochromatic) Wigner function of quantum optics to variable wavelength. In particular, we treated Gaussian beams and Schrödinger cat states.

The Lie-theoretical scaffold for this construction selects the polar parametrization of the group; this is associated with the Weyl operator-ordering rule of quantum mechanics [6]. Group parametrizations different from the polar form will lead to different distribution functions, such as the standard-, antistandard-, symmetrized, Born–Jordan, P-, Q-, and

Husimi functions [3]. The polar parametrization (and the Weyl ordering rule) is distinguished because the correspondence between c-numbers and wave operators under linear transformation is mantained [10,13].

The correspondence we propose between c-numbers and operators can be extended naturally beyond the Heisenberg–Weyl group of three parameters. On any N-parameter Lie group G we may establish a correspondence between $v_i \in \mathscr{R}$ and the N generators $\hat{X}_i$. The analogue of the formal operator (7) is

$$\mathscr{W}^G(v) = \int_G \mathrm{d}g(\gamma) \exp \mathrm{i} \sum_k \gamma_k \big(\hat{X}_k - v_k\big), \qquad (33)$$

where γ_i are the polar coordinates of the group and a Hilbert space of wavefunctions (on coset spaces of G) is defined with each model. The mother construction was applied to the Euclidean group for the 'wavefront' and Helmholtz models of optics in Ref. [7]; the Wigner function could be useful also for wide-angle acoustics.

Acknowledgements

For discussions and references for quantum and image optics I thank N.M. Atakishiyev, O. Castaños, S.M. Chumakov, A. Lohmann, J.L. Mateos, J. Ojeda-Castañeda in Mexico and J.D. Secada at ICIMAF, Cuba, on acoustics. Special mention is due to A.L. Rivera for providing the results displayed in Figs. 3 and 4 with the general-purpose software for Wigner functions from her doctoral dissertation. Support for the graphics is also acknowledged to G. Krötzsch. This work was performed under Project UNAM-DGAPA IN 106595 Optica Matemática.

References

[1] E. Wigner, Phys. Rev. 40 (1932) 749;
M. Hillery, R.F. O'Connell, M.O. Scully and E.P. Wigner, Phys. Rep. 106 (1984) 121.

[2] See e.g.: Y.S. Kim and M.E. Noz, Phase space picture in quantum mechanics, Lecture Notes in Physics Series, Vol. 40 (World Scientific, Singapore, 1991) ch. 3.

[3] H.-W. Lee, Phys. Rep. 259 (1995) 147.

[4] J.R. Klauder and E.C.G. Sudarshan, Fundamentals of Quantum Optics (Benjamin, Reading (Mass.), 1968).

[5] M.J. Bastiaans, J. Opt. Soc. Am. 69 (1979) 1710;
A. Lohmann, Optics Comm. 42 (1980) 32;
H.O. Bartelt, K.-H. Brenner and H. Lohmann, Optics Commun. 32 (1980) 32;
H. Bartelt and K.-H. Brenner, Israel J. Techn. 18 (1980) 260;
K.-H. Brenner and H. Lohmann, Optics Comm. 42 (1982) 310;
W. Schempp, C.R. Math. Rep. Ac. Sci. Canada 4 (1982) 43–48, 139–144, 219–224; 5 (1983) 121–126; 6 (1984) 179–182;
W.D. Furlan and G. Saavedra, Optics Comm. 96 (1993) 208;
J. Lancis, E.E. Sicre, E. Tajahuerce and P. Andrés, Appl. Optics (1996) in press;
N.M. Atakishiyev, S.M. Chumakov, A.L. Rivera and K.B. Wolf, Phys. Lett. A 215 (1996) 128.

[6] K.B. Wolf, The Heisenberg–Weyl ring in quantum mechanics, in: Group Theory and its Applications, III, Ed. E.M. Loebl (Academic Press, New York, 1975) pp. 189–247.

[7] K.B. Wolf, Kinam 6 (1984) 141;
Elements of Euclidean optics, in: Lie Methods in Optics, Lecture Notes in Physics, Vol. 352 (Springer Verlag, Heidelberg, 1989) ch. 6, pp. 115–162;
The Euclidean mother group of geometric and wave optics, in: Procs. 4th Wigner Symp. (World Scientific, Singapore, 1996) pp. 194–202.

[8] M. Moshinsky and C. Quesne, Oscillator systems, in: Procs. 15th Solvay Conf. in Physics (1970) (Gordon and Breach, New York, 1974); J. Math. Phys. 12 (1971) 1772; J. Math. Phys. 12 (1971) 1780.

[9] M. Kauderer, Symplectic matrices, First order systems and special relativity (World Scientific, Singapore, 1994.)

[10] G. García-Calderón and M. Moshinsky, J. Phys. A 13 (1980) L185.

[11] V.V. Dodonov, L.A. Malkin and V.I. Man'ko, Physica 72 (1974) 597;
B. Yurke and D. Stoler, Phys. Rev. Lett. 57 (1986) 13;
V.I. Man'ko, Photon statistics for multimode squeezed Schrödinger cat states, in: Quantum-like Models and Coherent Effects, Eds. R. Fedele and P.K. Shukla (World Scientific, Singapore, 1995);
O. Castaños, R. López-Peña and V.I. Man'ko, Schrödinger cat states of the nonstationary generalized oscillator, in press.

[12] S.M. Chumakov and K.B. Wolf, Phys. Lett. A 193 (1994) 51.

[13] M. García-Bullé, W. Lassner and K.B. Wolf, J. Math. Phys. 27 (1986) 29.